INTERACTION OF INTENSE ULTRASHORT VUV PULSES WITH DIFFERENT SOLIDS

RESULTS FROM THE TESLA TEST FACILITY *FEL* PHASE I

Jacek Krzywinski

Institute of Physics, Polish Academy of Sciences and Deutsches Elektronen-Synchrotron DESY

26TH INTERNATIONAL
FREE ELECTRON LASER CONFERENCE
& 11TH FEL USERS WORKSHOP

fel 2004
AUGUST 29 - SEPTEMBER 3
Trieste, Italy

FELIS

Free Electron Laser - Interaction with Solids

A. Andrejczuk [1,4,] [+] M. Bittner [+]D. Chvostova, F.Felten [9],U. Hahn [2], S. Jacobi [8], M. Jurek [1], [+]L.Juha,, A.Kauch[3], [+]J . Krasa, J.Krzywinski, V.Letal, [1,2], J.B. Pelka [1], H. Reniewicz[4],. W. Sobala [5], R. Sobierajski [2,6], B. Steeg[2], [+] V. Vorlicek ,, A.Wawro and TTF FEL team

[1]Institute of Physics, Polish Academy of Sciences, Poland, ,[+] Institute of Physics, Czech Academy of Sciences, Czech Republic, [2]HASYLAB at DESY, Germany, [3]Warsaw University, Poland, [4]University of Bialystok, Poland, [5]Institute of Nuclear Physics, Cracow, Poland, [6]Warsaw University of Technology, Poland,, [8]GKSS Research Center,Germany, [9]Harburg-Hamburg Technical University

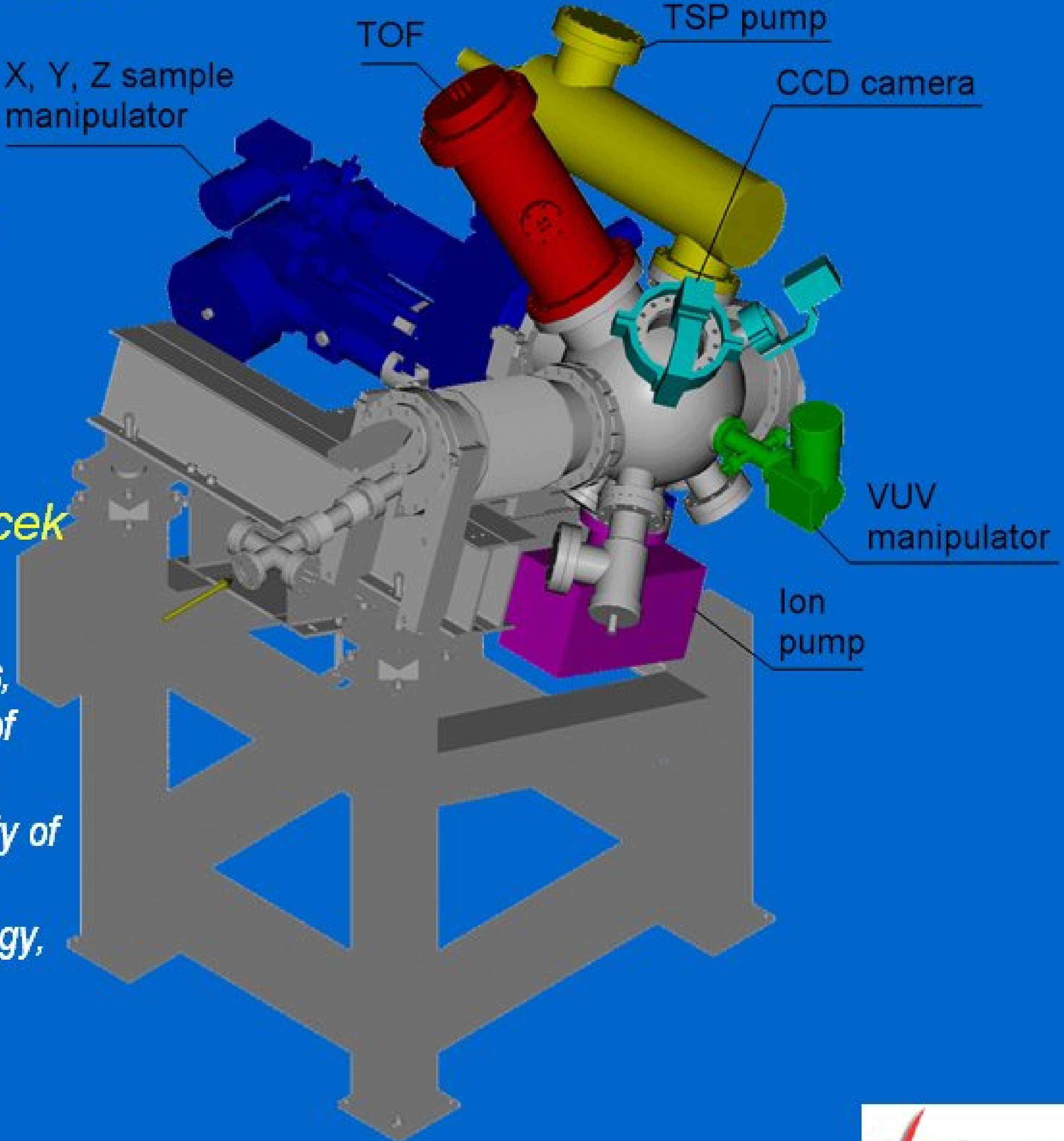

Outline:

- Motivation
- Experimental
- Damage and surface modification – short introduction
- Results
- Conclusions

Why XUV/x-ray ablation should be investigated?

1. estimating and minimizing **damages to surfaces of heavily loaded XUV/x-ray optical elements** developed and used for guiding and focusing of short-wavelength laser beams

2. durability assessments of materials suggested for the **first walls of ICF reactors** and optical elements exposed to intense XUV/x-ray radiation in a laser-plasma interaction chamber

3. diffraction-limited **nanostructuring** of solid surfaces for fabrication of **microelectronic and micromechanical elements** and devices

4. determination of radiation field characteristics: imaging of spatial energy distribution in a focused beam ablatively imprinted on the irradiated material and determination of pulse energy content

Absorption of visible and VUV radiation

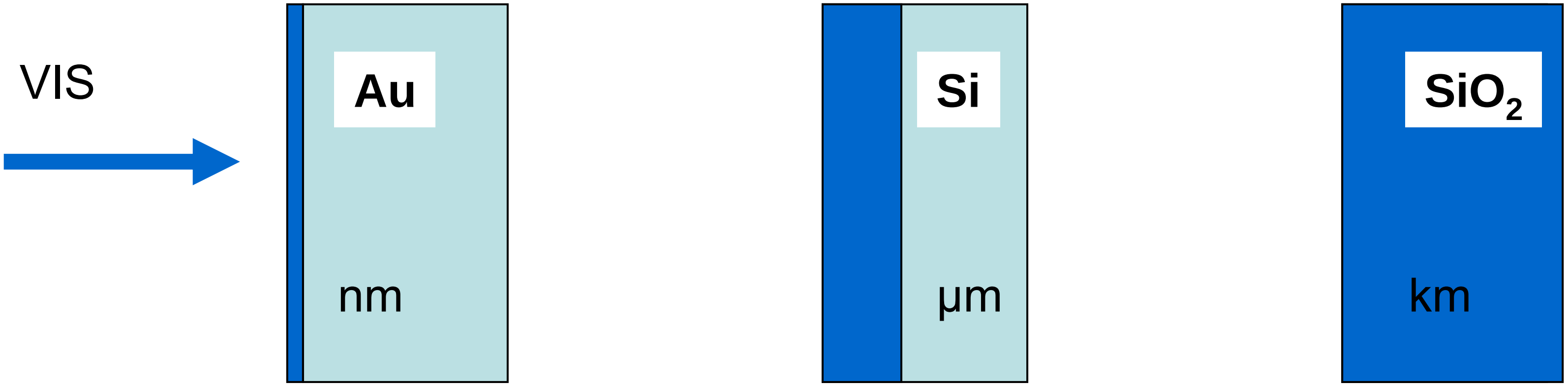

VIS

Au nm

Si µm

SiO_2 km

For a first time it was possible to excite surfaces of metals, semiconductors, insulators in the very similar way: linear absorption, similar absorption coefficient

and concentrate on the following question:

How different materials respond to a similar excitation?

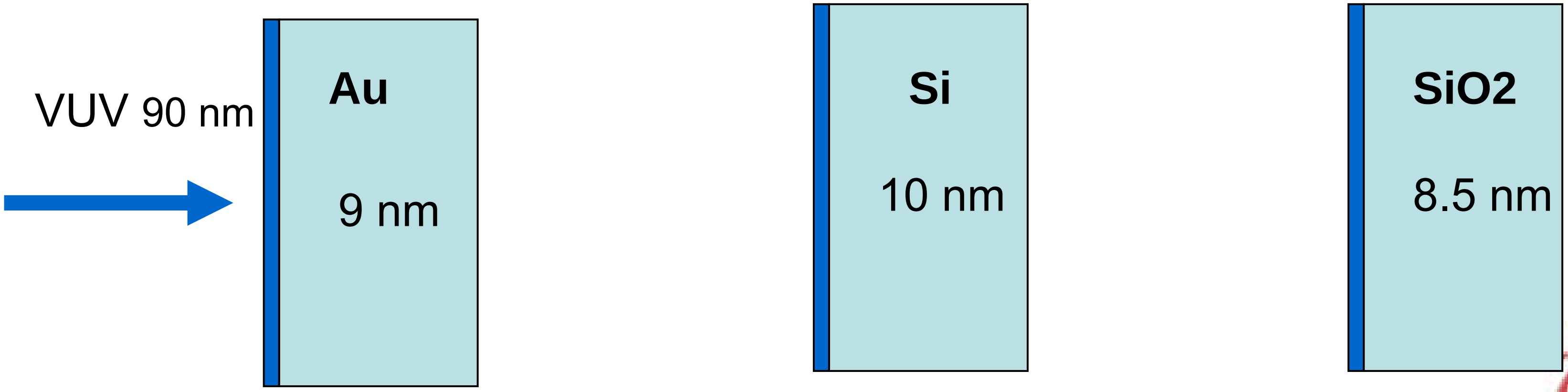

VUV 90 nm

Au 9 nm

Si 10 nm

SiO2 8.5 nm

Layout of the experiment

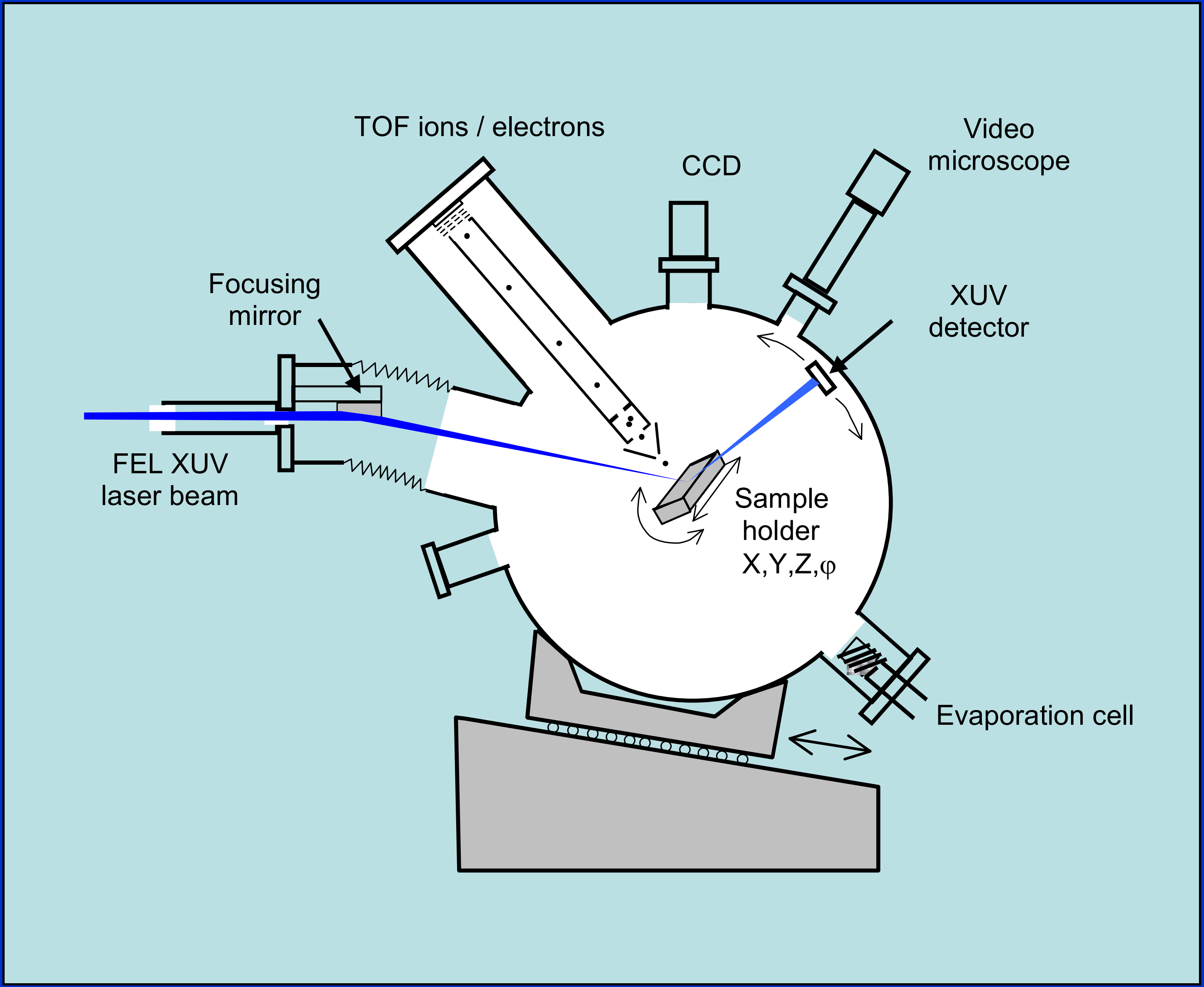

Photon Beam Parameters

Wavelength	86-98 nm
Pulse length	50 fs
Pulse energy	1-0 uJ
Min. Spot size	10 um
Max. Intensity	~10^{14} W/cm^2

Samples

Metals:
Au, Al, Cu
Semiconductors
Si, a-C
Insulators
Al_2O_3 SiO_2 YAG
MgF_2 BaF_2
Organic compounds
PMMA, PTFE

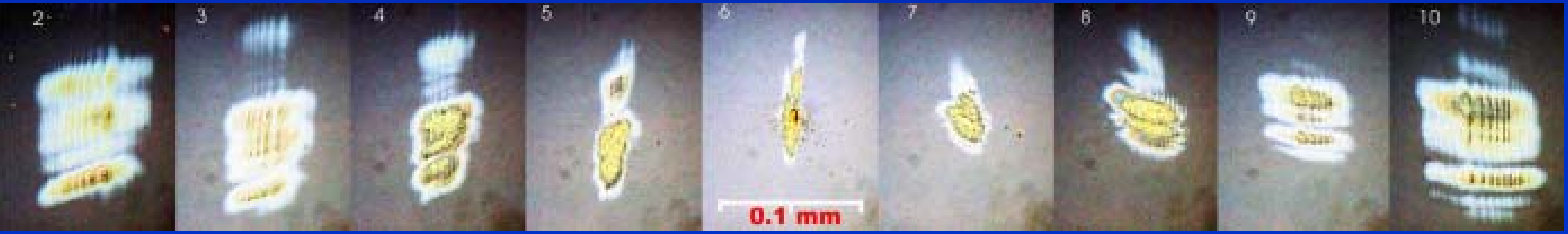

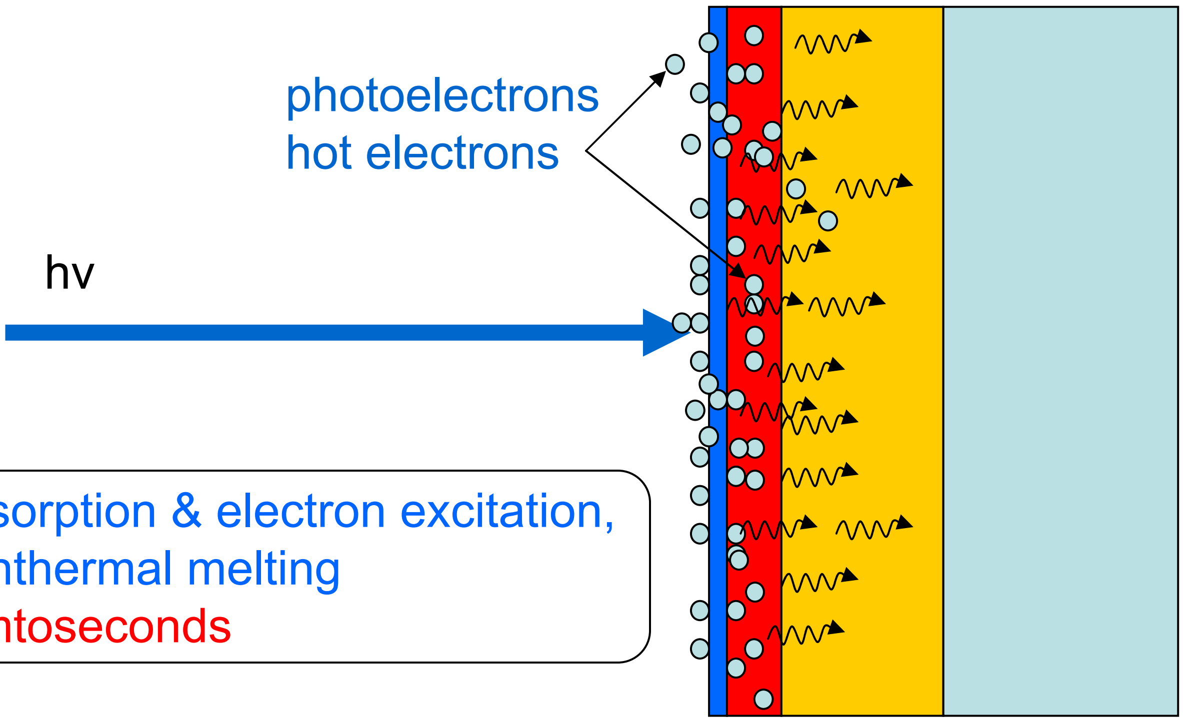

photoelectrons
hot electrons

hv

absorption & electron excitation,
nonthermal melting
femtoseconds

electron difussion & thermalization,

thermal melting, evaporation

picoseconds

heat difiussion, ablation front propagation

nanoseconds

Example of theoretical predictions: Au

Photon beam

hν = 14 eV
λ= 86 nm

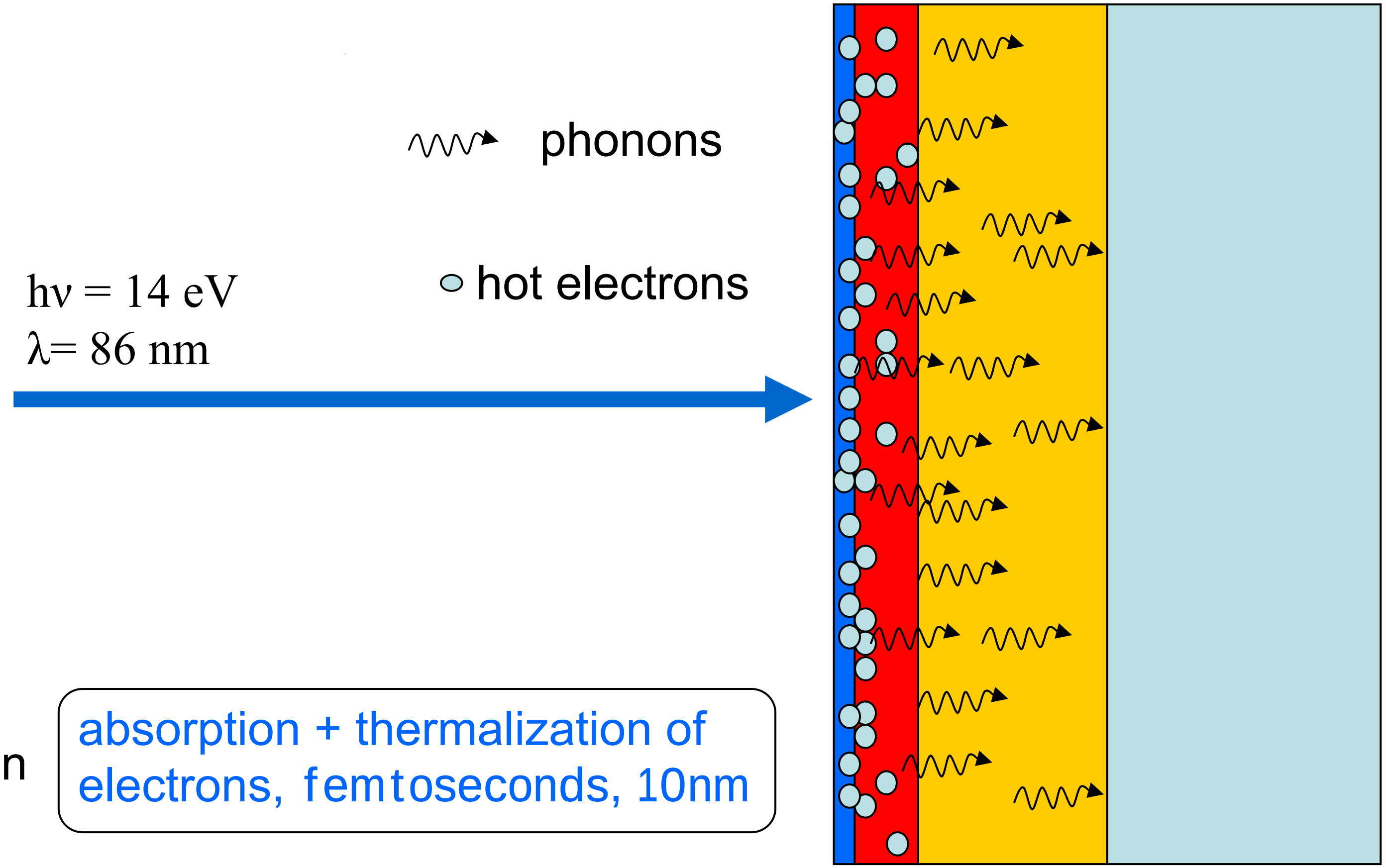

phonons

hot electrons

Boltzman equation

absorption + thermalization of electrons, femtoseconds, 10nm

Two temperature model

Hot electrons diffusion → phonons
picoseconds, 100 nm

Hydronynamical code: XUV – Ablator,

Lagrangian finite-difference method, Mie-Grüneisen equation of state (EOS) based on the code developed by T. Anderson:. PhD thesis, University of California at Berkeley, 1996 and modified by V. Letal, L. Juha, A. M. Bittner, J. Krzywinski, J. R. Sobierajski)

Heat diffiusion by phonons,
Pressure wave propagation
nanoseconds, 1000 nm

Thermalization of electron gas in metals e-e and e-ph scattering (R.Sobierajski)

Time constant **τ** depends on energy deposition

For energy deposition ~ 1 eV/ atom τ~ 5 fs

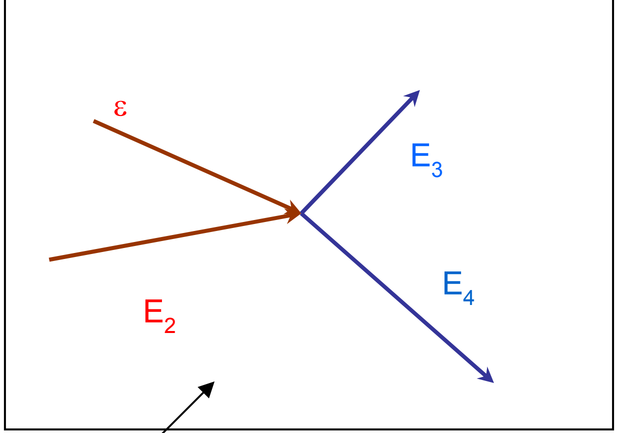

collision integrals

$$\frac{dn(\varepsilon)}{dt} = C_{e-e}[n(\varepsilon)] + C_{e-f}[n(\varepsilon)]$$

Boltzman equation

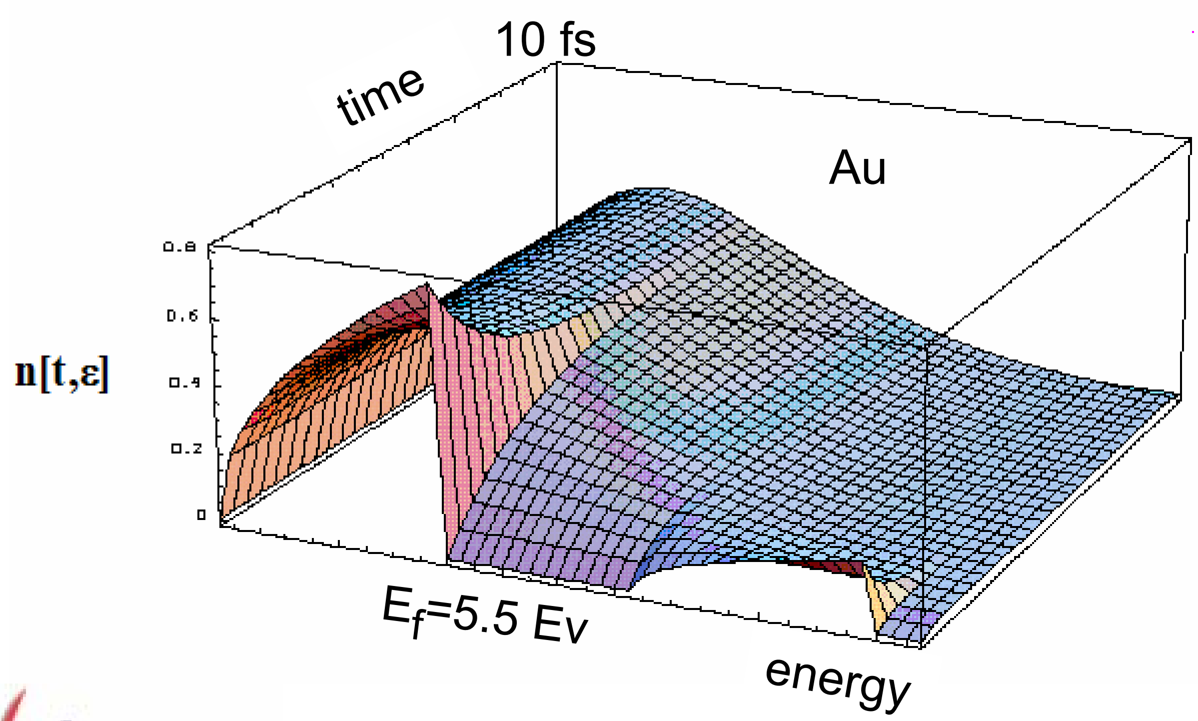

Electron distribution can be described by temperature for t > 5fs

Two temperature model: Au

$$\begin{cases} C_e(T_e)\dfrac{\partial T_e}{\partial t} = \kappa(T_e,T_i)\cdot\nabla^2 T_e - G(T_e,T_i) + P(t,\vec{r}) \\ C_i(T_i)\dfrac{\partial T_i}{\partial t} = +G(T_e,T_i) \end{cases}$$

T_e, T_i temperature of electrons and ions

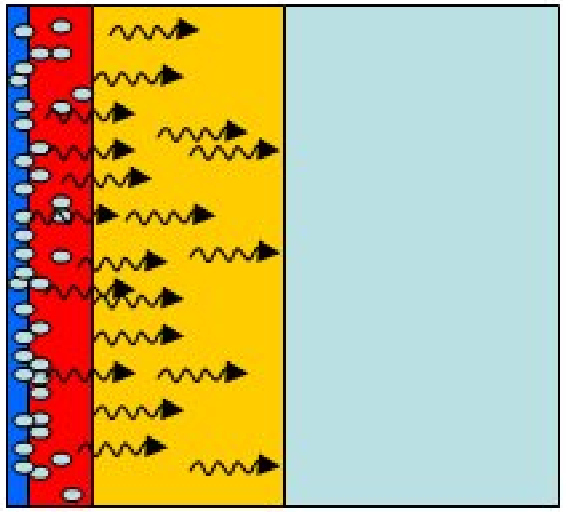

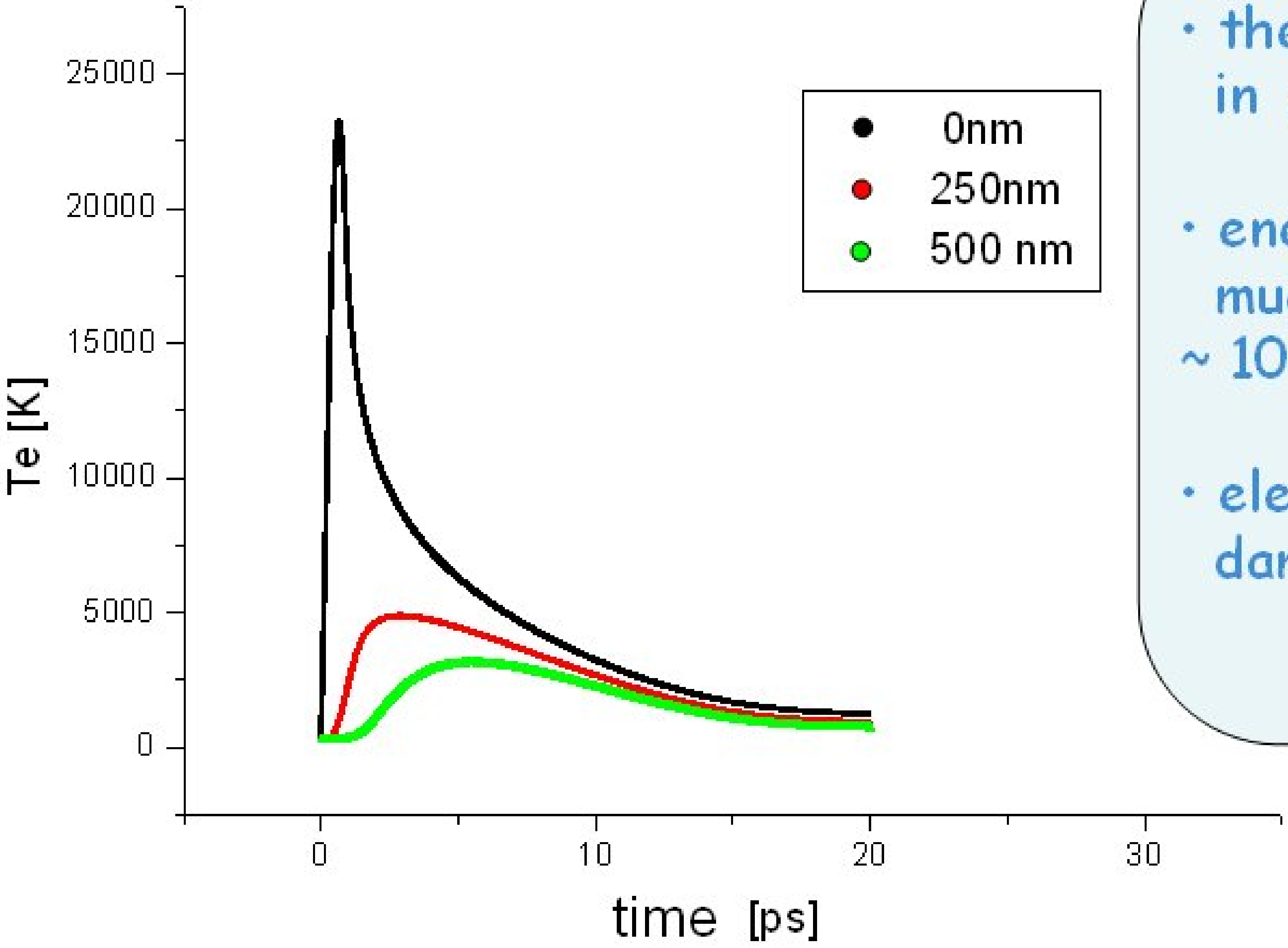

- thermalisation of hot electrons in picosecond scale
- energy penetration depth ~100nm much larger than absorption depth ~ 10 nm
- electron difussion should increase damage threshold

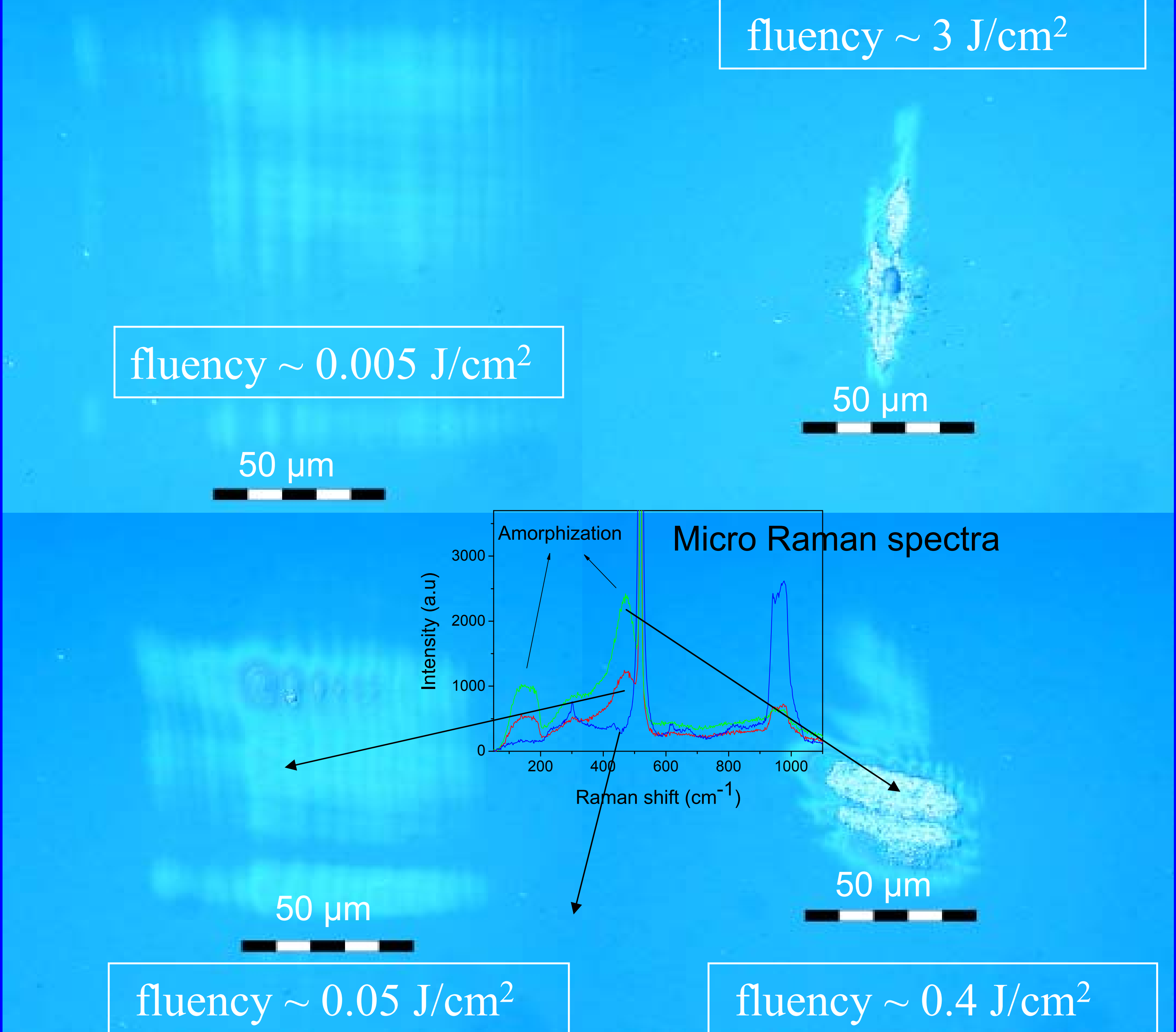

fluency ~ 3 J/cm^2

fluency ~ 0.005 J/cm^2

Micro Raman spectra

fluency ~ 0.05 J/cm^2

fluency ~ 0.4 J/cm^2

Table 1: Surface modification thresholds

Sample	**ΦI** [J/cm^2]	**ΦII** [J/cm^2]
Au	0.02	0.02
Au-15	0.01	0.01
a-C-40	0.01	0.03
Si	0.005	0.04
SiO_2	0.03	0.03
Ce:YAG	0.02	0.02
PMMA	0.01	0.01

ΦI is the fluency at which we notice the change of the refractive index

ΦII is the fluency at which we notice the deformation of the surface detected by AFM.

It is interesting to notice, (that except for the Au-10 and the PMMA) the ΦII values oscillate around 0.03 J/cm^2 This number is in the order of the fluency F_{coh} at which the absorbed energy per atom is equal to the cohesion energy E_{coh}: $F_{coh} = E_{coh} \cdot n / \alpha$ where n is the concentration and α is the absorption coefficient.

For typical values: E_{coh}~3 eV, n~$5 \cdot 10^{22}$, and α~10^6 cm-1

F_{coh}~0.025 J/cm^2 corresponds to the **measured value.**

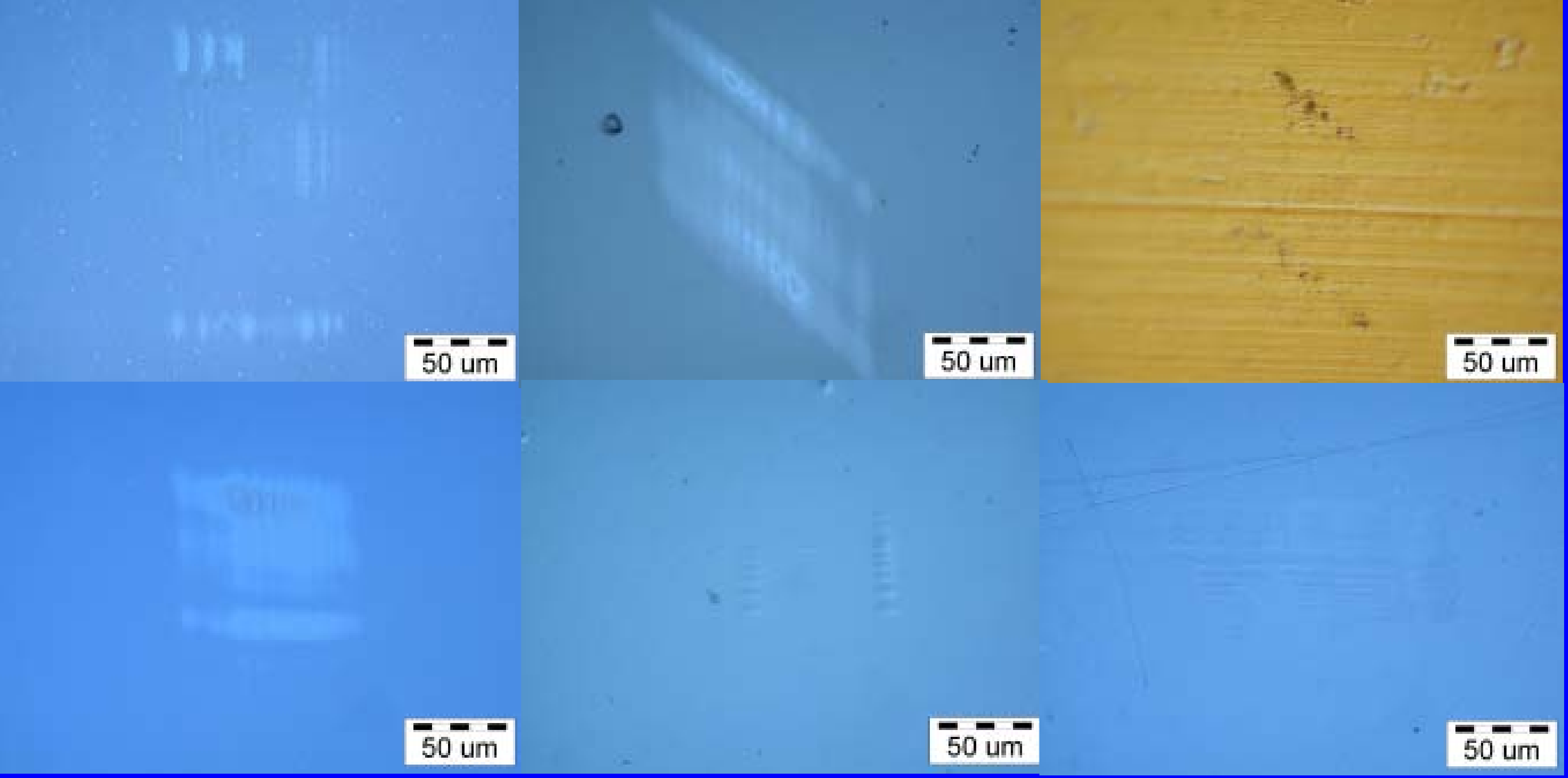

It is interesting to notice, (that except for the Au-10 and the PMMA) the ΦII values oscillate around 0.03 J/cm^2 This number is in the order of the fluency Fcoh at which the absorbed energy per atom is equal to the cohesion energy Ecoh: $F_{coh} = E_{coh} \cdot n / \alpha$ where n is the concentration and α is the absorption coefficient.

For typical values:

$E_{coh} \sim 3$ eV, $n \sim 5 \cdot 10^{22}$, and $\alpha \sim 10^{6}$ cm-1 $F_{coh} \sim 0.025$ corresponds to the measured value.

Stress related damage

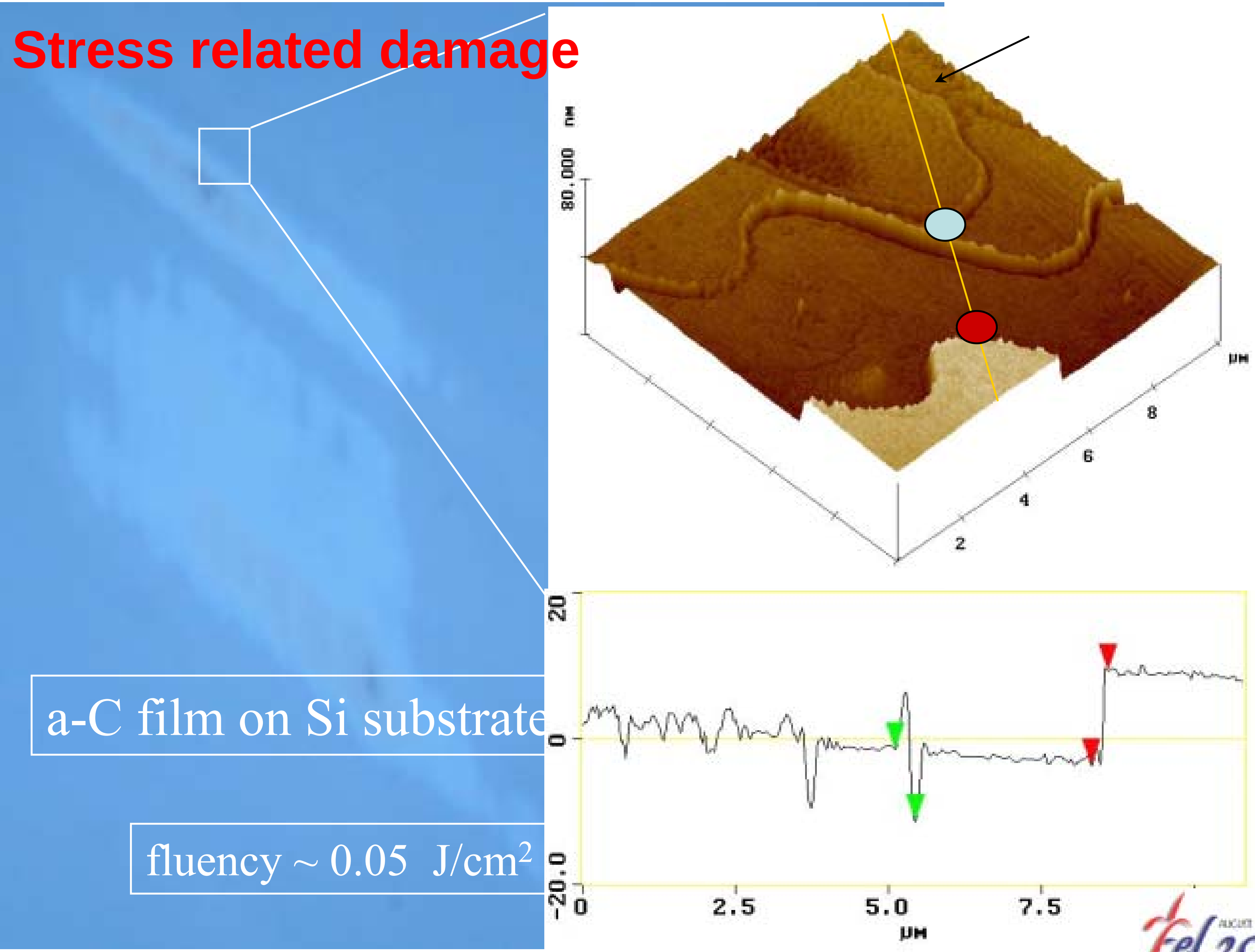

a-C film on Si substrate

fluency ~ 0.05 J/cm^2

Multi-shot modification of silicon and quartz surfaces

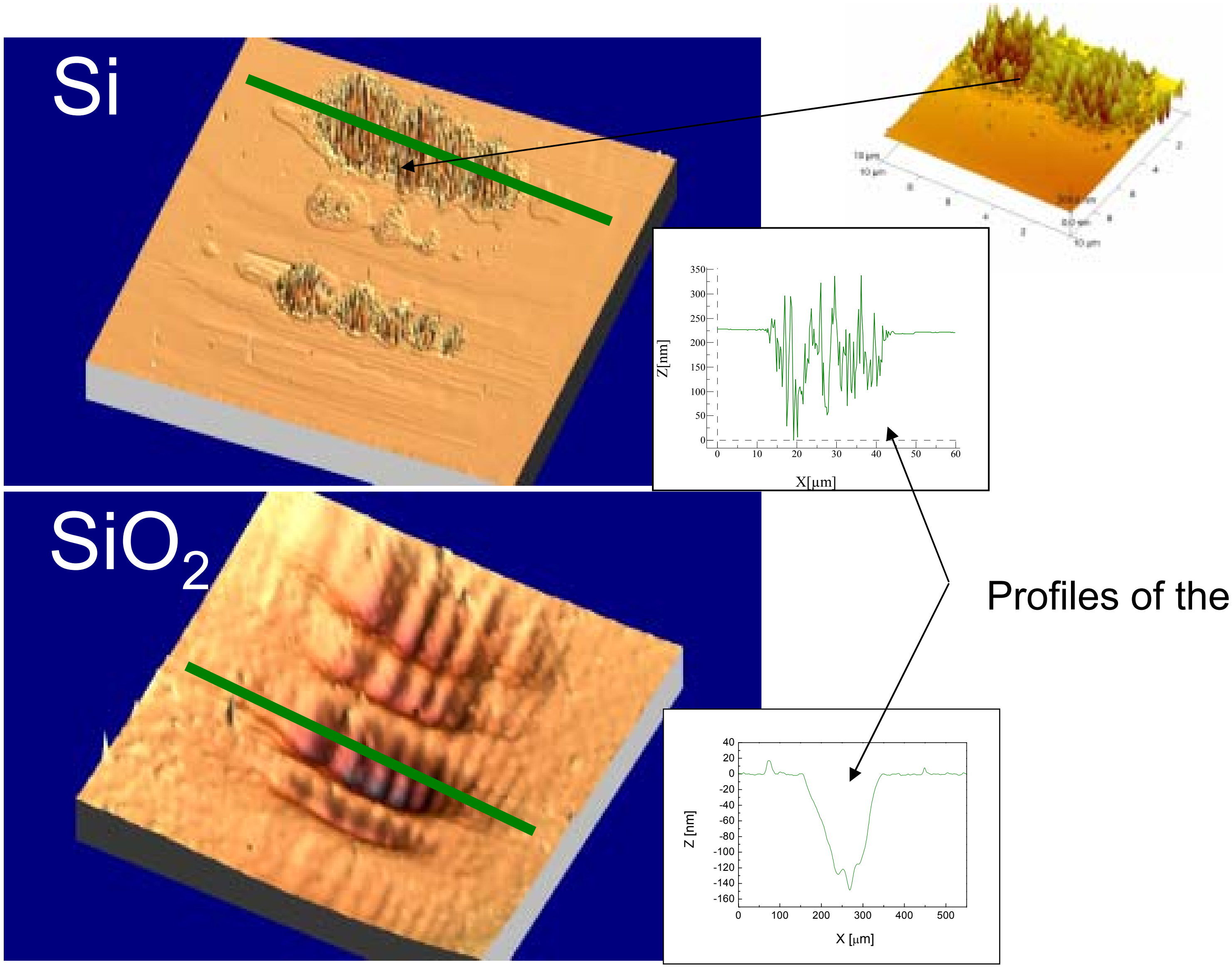

Profiles of the craters

Spallation depth were calculated with a help of the XUV ABLATOR hydrodynamic code

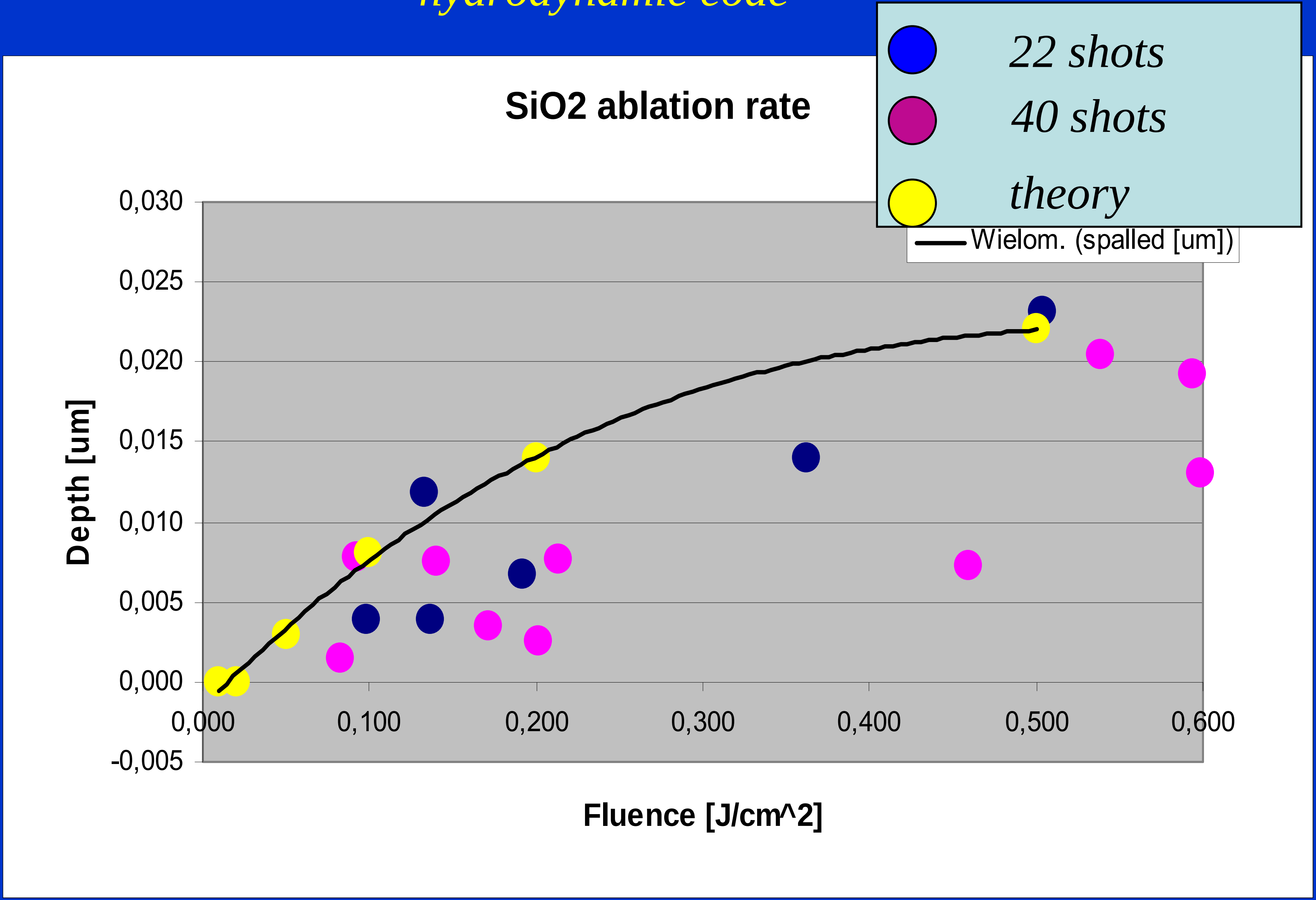

Printing interference pattern into surfaces of different insulators

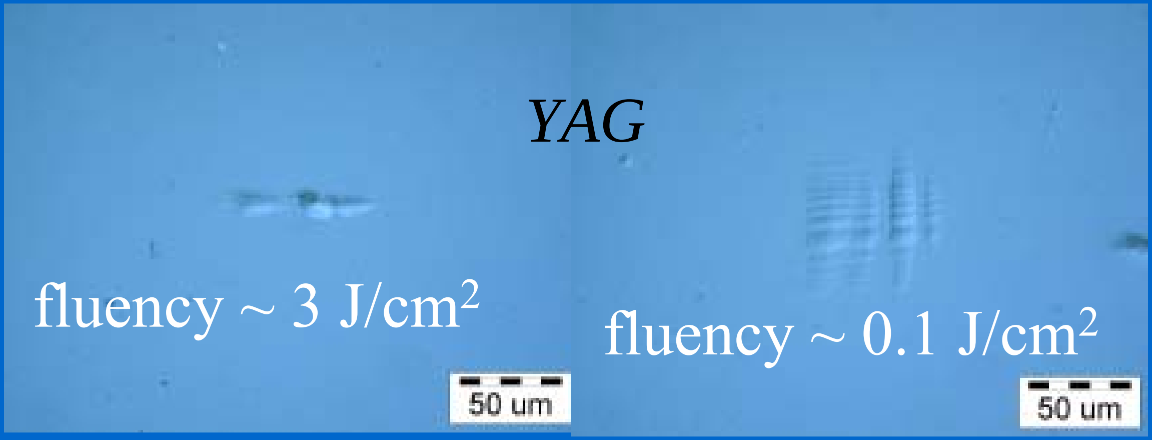

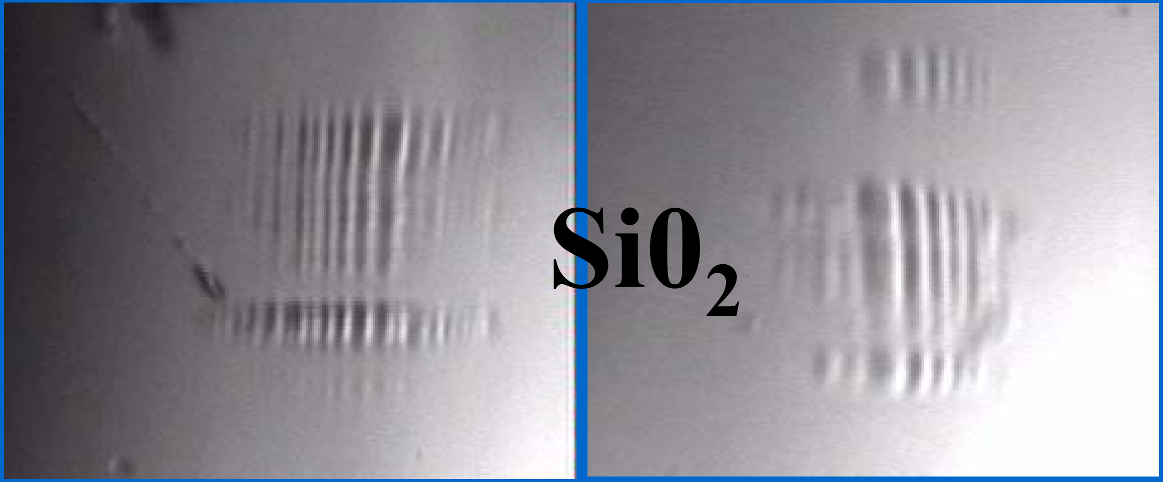

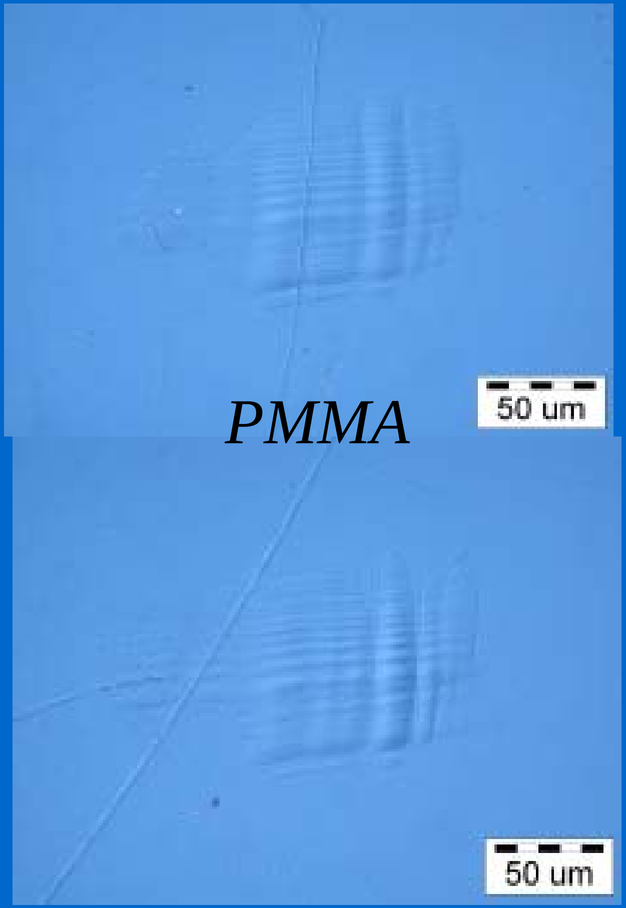

Very „clean" ablation. Edges of the craters are sharp, no cracks, debris, column structures. It was easy to drill a nice holes trough the samples (SiO_2, BaF_2) Morphology of the craters' interior hardly depends on the applied fluency.

Ion emission for conducting and insulating materials

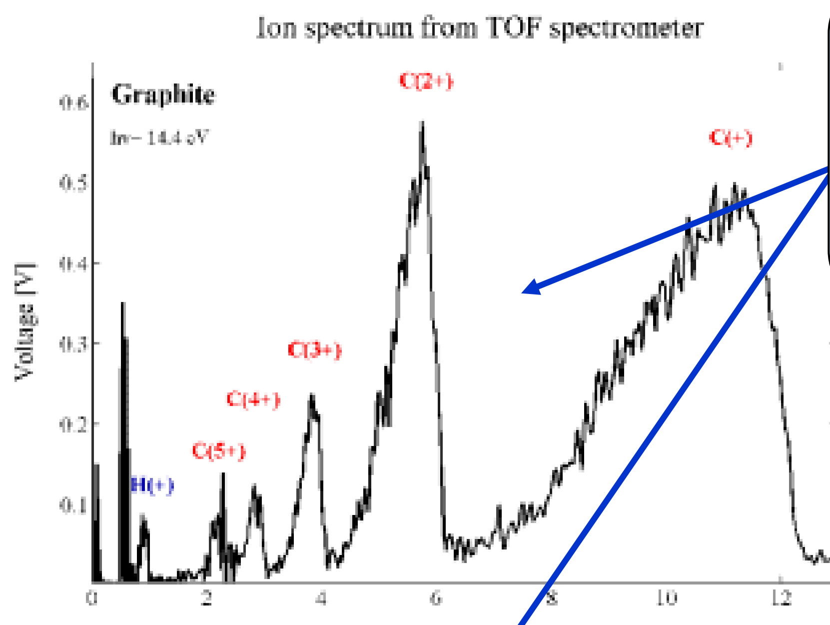

High charge states and energetic ions (~a few keV) were typical for conductors and semiconductors.
Ion energu ~charge → field emissionn

Only single ions states and low energetic ions (~50 eV) were detected for insulators for all irradiation conditions.

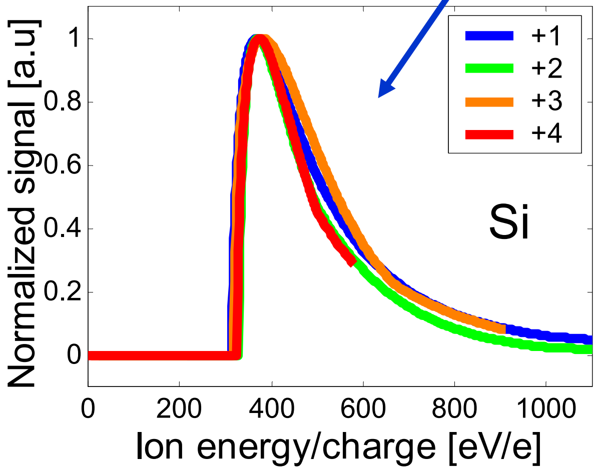

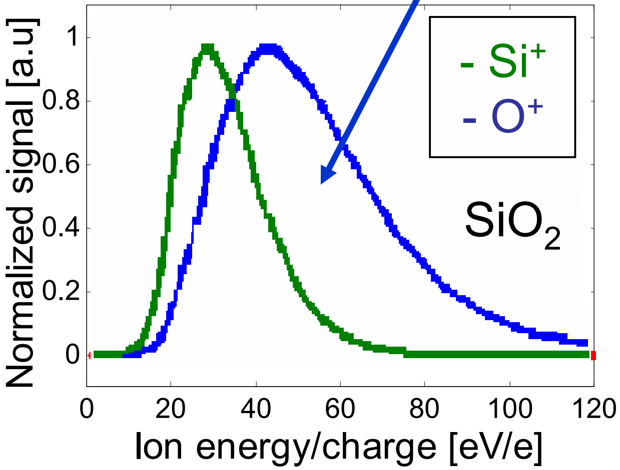

LIPSS = spontaneously-grown periodical structures on the laser-illuminated surfaces

(spatial period of the structures is usually related to the laser laser wavelength)

LIPSS in PMMA
$267\ \mathrm{nm} < \Lambda < 413\ \mathrm{nm}$

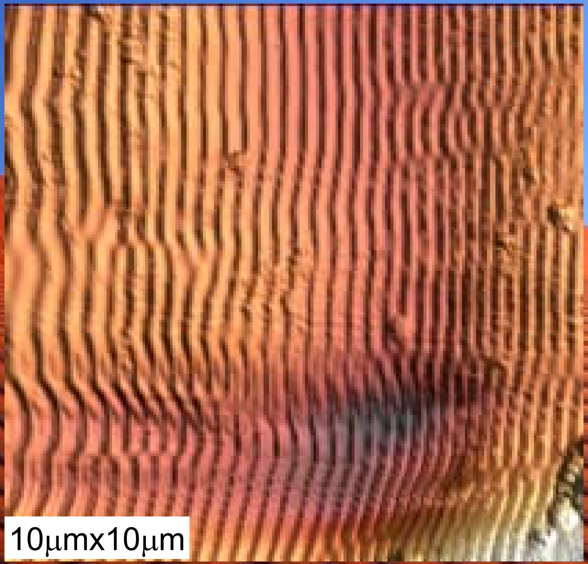

Can we find LIPSS with a period correlated to the irradiation wavelength?

Does the wavelength always control the LIPSS period?

1. Can we find LIPSS with a period correlated to the irradiation wavelength?

Answer for the first question is : yes!, the period is 80 nm

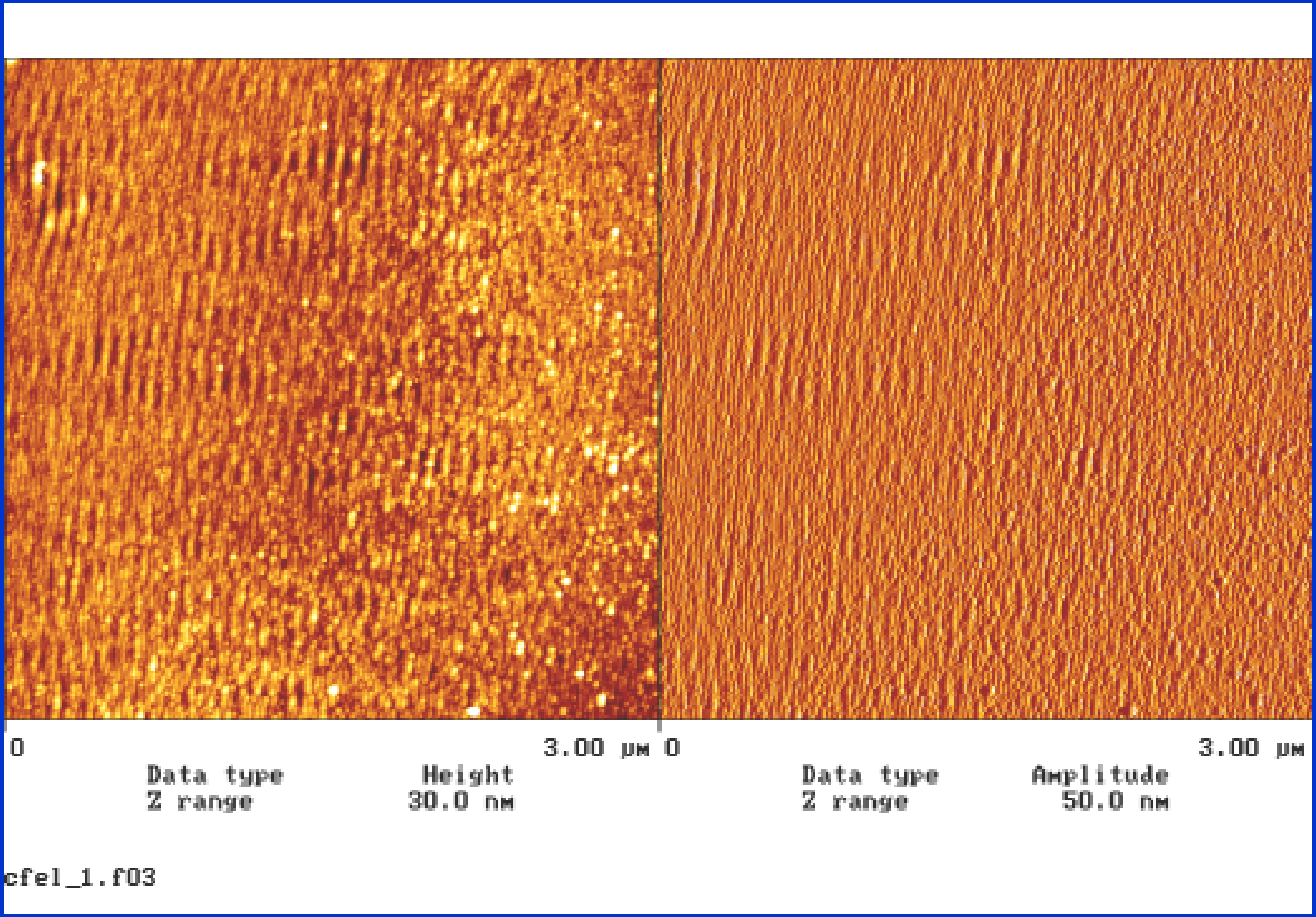

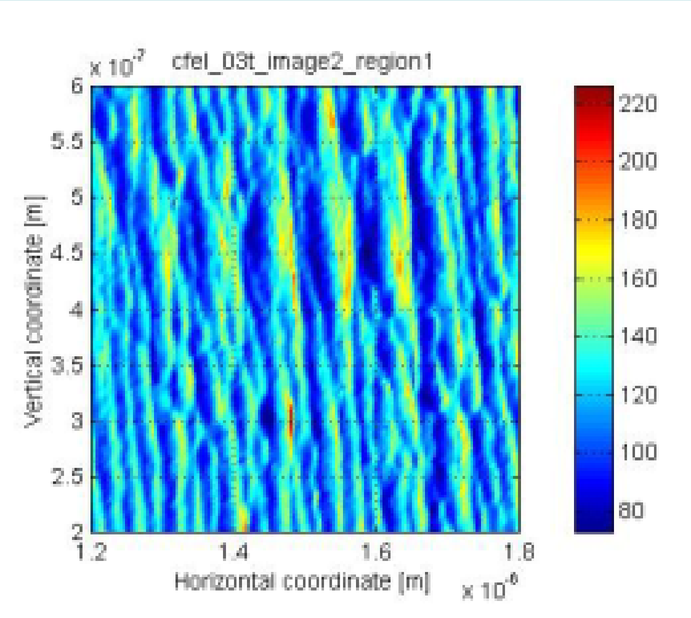
cfel_03t_image2_region1
x 10^-7
Vertical coordinate [m]
6
5.5
5
4.5
4
3.5
3
2.5
2
Horizontal coordinate [m]
1.2
1.4
1.6
1.8
x 10^-6
220
200
180
160
140
120
100
80

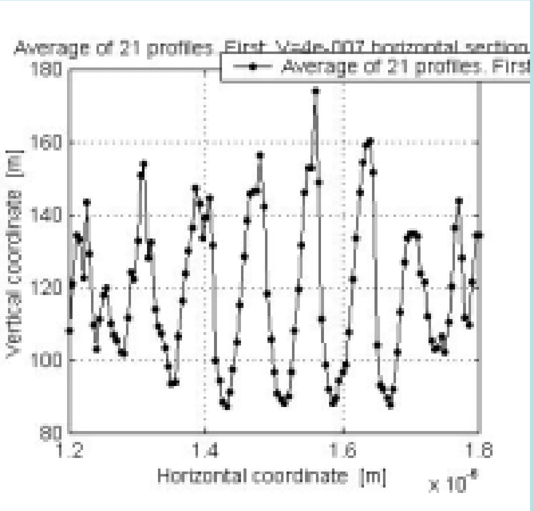
Average of 21 profiles. First: V=4e-007 horizontal section
Average of 21 profiles. First
Vertical coordinate [m]
180
160
140
120
100
80
Horizontal coordinate [m]
1.2
1.4
1.6
1.8
x 10^-6

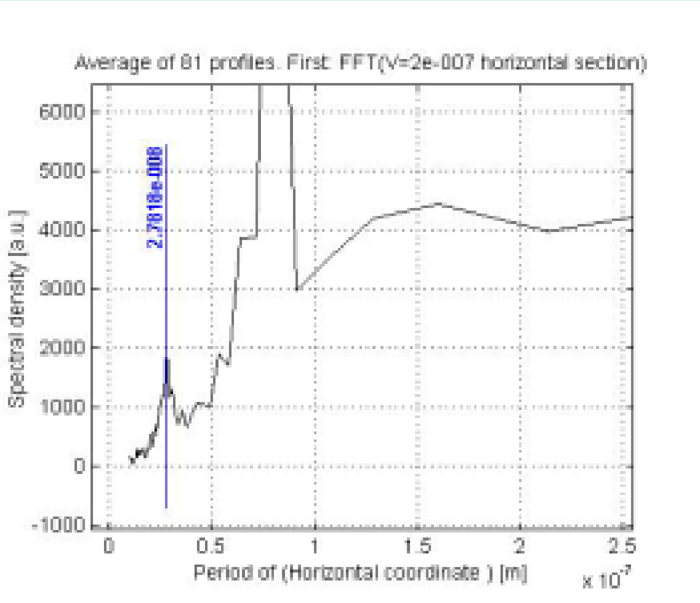
Average of 81 profiles. First: FFT(V=2e-007 horizontal section)
2.7818e-008
Spectral density [a.u.]
6000
5000
4000
3000
2000
1000
0
-1000
Period of (Horizontal coordinate) [m]
0
0.5
1
1.5
2
2.5
x 10^-7

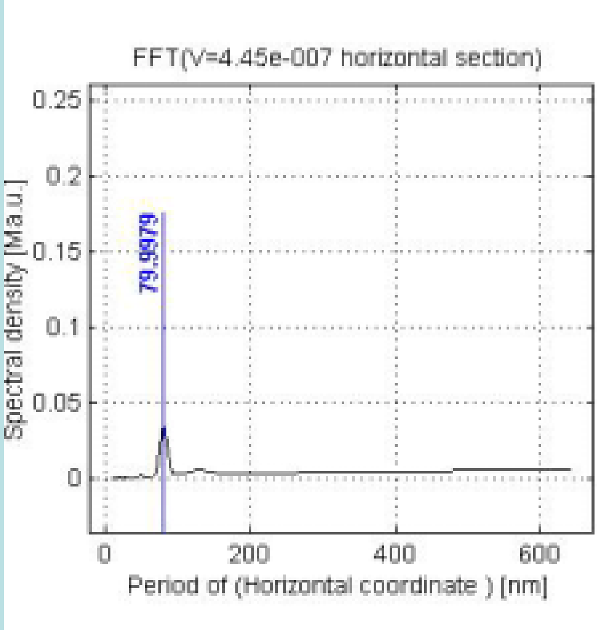
FFT(V=4.45e-007 horizontal section)
79.9979
Spectral density [Ma.u.]
0.25
0.2
0.15
0.1
0.05
0
Period of (Horizontal coordinate) [nm]
0
200
400
600

Does the wavelength only control the LIPSS period? Clearly, in most cases, not!

Craters ablated before, behind, and exactly at the tight focus position.

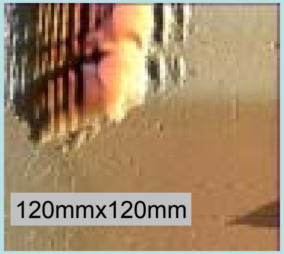

increasing fluence

LIPSS-II of the second kind induced at the bottom of craters ablated in PMMA at increasing fluency.

The spatial period increases with fluency.

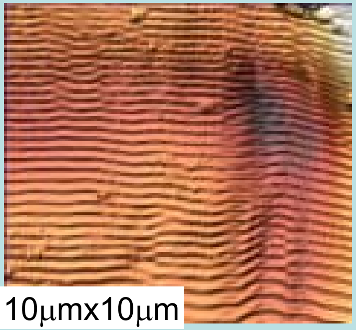

LIPSS-II in PMMA
$267 \text{ nm} < \Lambda < 413 \text{ nm}$

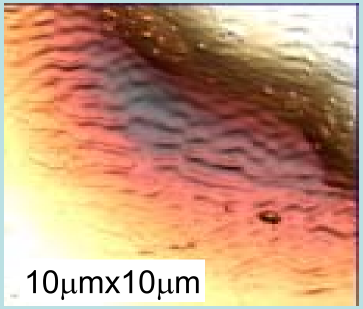

LIPSS-II in PMMA
$600 \text{ nm} < \Lambda < 700 \text{ nm}$

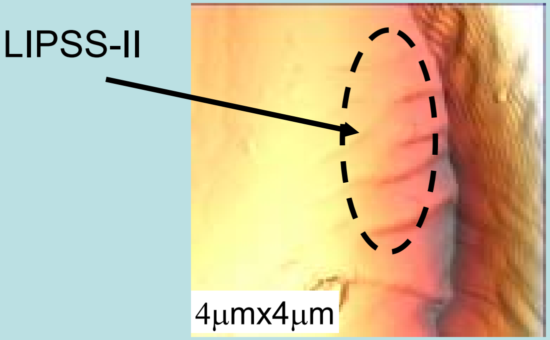

LIPSS-II in PMMA
$500 \text{ nm} < \Lambda < 1000 \text{ nm}$

Conlussion 1

- Measured damage threshold for all investigated materials was estimated to be between 10 - 40 mJ/cm^2
- This value corresponds well to the fluency at which the absorbed energy per atom is equal to the cohesion energy.
- The result is surprising in case of bulk metals. One expects that hot electrons should take most of the deposited energy from away the absorption volume and thus increase the threshold value.

Conclussion 2

- **A distinct difference in the behavior of conducting materials and insulators was observed. The difference is dramatic while the absorption coefficients are similar for all the materials at the TT1 FEL wavelength.**
  - For insulators the ablation is very „clean”. Edges of the craters are sharp, no cracks, debris, column structures. Morphology of the craters' interior hardly depends on the applied fluency. Ablation rate agrees with hydrodynamic simulations.
  - In contrast, the irradiated silicon surface becomes very rough when the intensity exceeds the damage threshold.
  - There was also a clear difference between insulators and conducting material with respect to ejected ions spectra. High charge states and energetic ions (~a few keV) were typical for conductors and semiconductors. Only single ions states and low energetic ions (~50 eV) were detected for insulators for all irradiation conditions.

Conclusion 3

- **LIPSS-I have been found at the rim of a few craters created in a-C and PMMA by 98-nm and 86-nm radiation, respectively.**

- **LIPSS of the second kind (LIPSS-II) has also been found. LIPSS-II spatial periods depend more on laser intensity than wavelength and are significantly longer than the laser wavelength. Very common phenomenon.**

Time resolved ablation /transmission mesurements for TTF FEL2

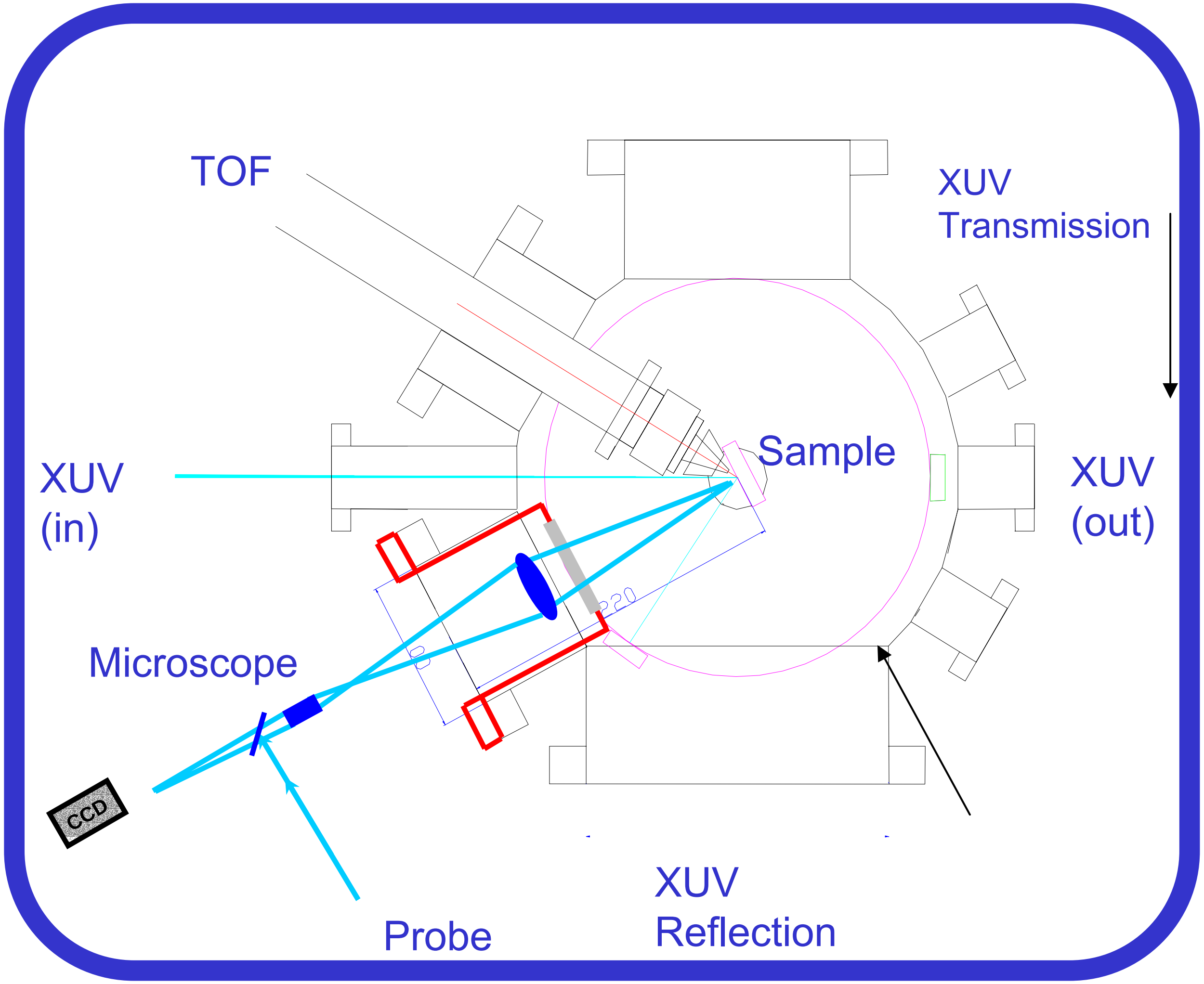

- The VUV R can be rotated (in the theta – two theta mode) and can be set in front of the VUV T. This feature allows calibration of both devices with respect to each other.